

Cardiac Resynchronization Therapy Homogenizes Myocardial Glucose Metabolism and Perfusion in Dilated Cardiomyopathy and Left Bundle Branch Block

Bernd Nowak, MD,* Anil M. Sinha, MD, PhD,† Wolfgang M. Schaefer, MD, PhD,* Karl-Christian Koch, MD,† Hans-Juergen Kaiser, PhD,* Peter Hanrath, MD, FACC,† Udalrich Buell, MD,* Christoph Stellbrink, MD†

Aachen, Germany

OBJECTIVES	We investigated whether cardiac resynchronization therapy (CRT) affects myocardial glucose metabolism and perfusion in dilated cardiomyopathy (DCM) and left bundle branch block (LBBB).
BACKGROUND	Patients with DCM and LBBB present with asynchronous left ventricular (LV) activation, leading to reduced septal glucose metabolism. Cardiac resynchronization therapy recoordinates LV activation, but its effects on myocardial glucose metabolism and perfusion remain unknown.
METHODS	In 15 patients (10 females; 61 ± 13 years) with DCM and LBBB (QRS width 165 ± 15 ms), gated ^{18}F -fluorodeoxyglucose (FDG) positron emission tomography (PET) and technetium-99m ($^{99\text{m}}\text{Tc}$)-sestamibi single-photon emission computed tomography were performed before and after two weeks of CRT. Uptake of FDG and $^{99\text{m}}\text{Tc}$ -sestamibi was determined in four LV wall areas. Ejection fraction and volumes were calculated from gated PET.
RESULTS	Baseline FDG uptake was heterogeneous ($p < 0.0001$), with lowest uptake in the septal region ($56 \pm 12\%$) and highest uptake in the lateral region ($89 \pm 6\%$). During CRT, septal and anterior increases ($p < 0.01$) and lateral decreases ($p < 0.01$) resulted in homogeneously distributed glucose metabolism. Baseline heterogeneity ($p < 0.0001$) in $^{99\text{m}}\text{Tc}$ -sestamibi uptake was modest (lowest septal $65 \pm 10\%$; maximum lateral $84 \pm 5\%$) and also reduced with CRT, although some heterogeneity ($p < 0.05$) remained. The septal-to-lateral ratio increased with CRT for FDG (0.62 ± 0.12 to 0.91 ± 0.26 , $p < 0.001$) and $^{99\text{m}}\text{Tc}$ -sestamibi uptake (0.77 ± 0.13 to 0.85 ± 0.16 , $p < 0.01$). The LV end-diastolic and end-systolic volumes decreased from 293 ± 160 to 272 ± 158 ml ($p < 0.05$) and from 244 ± 164 to 220 ± 160 ml ($p < 0.01$), respectively. Ejection fraction increased from $22 \pm 12\%$ to $25 \pm 13\%$ ($p < 0.01$).
CONCLUSIONS	Glucose metabolism is reduced more than perfusion in the septal compared with LV lateral wall in patients with DCM and LBBB. Cardiac resynchronization therapy restores homogeneous myocardial glucose metabolism with less influence on perfusion. (J Am Coll Cardiol 2003;41:1523–8) © 2003 by the American College of Cardiology Foundation

Patients with heart failure (HF) due to dilated cardiomyopathy (DCM) frequently present with left bundle branch block (LBBB), causing delayed activation of the left ventricle (LV). Experimental data indicate that LV activation delay is associated with reduced septal glucose metabolism (1). This experimental observation was recently confirmed in humans with DCM and LBBB (2). Early septal contraction against a relaxed LV, with resultant decreasing adenosine triphosphate requirements, is discussed as the pathophysiologic correlate (3). Reports on resting septal perfusion in patients with LBBB are contradictory. They range from diminished to normal perfusion, as estimated with thallium-201 or technetium-99m ($^{99\text{m}}\text{Tc}$) compounds with single-

photon emission computed tomography (SPECT) or ^{13}N -ammonia positron emission tomography (PET) (2,4–8).

Cardiac resynchronization therapy (CRT) recoordinates ventricular activation by atrial synchronous left or biventricular pacing. Hemodynamic improvement with CRT has been demonstrated in HF patients with LBBB (9,10). However, the effects of CRT on regional myocardial glucose metabolism and perfusion remain unknown.

Gated PET using ^{18}F -fluorodeoxyglucose (FDG) enables noninvasive measurement of myocardial glucose metabolism and calculation of LV volumes and ejection fraction (LVEF), whereas myocardial perfusion can be measured by $^{99\text{m}}\text{Tc}$ -sestamibi SPECT. Thus, the aim of the present study was to investigate whether the hemodynamic benefit of short-term CRT is paralleled by normalization of the unbalanced regional myocardial glucose metabolism and whether CRT affects regional myocardial perfusion in patients with DCM and LBBB.

From the Departments of *Nuclear Medicine and †Internal Medicine I (Cardiology), University Hospital, Aachen University of Technology, Aachen, Germany.

Manuscript received September 17, 2002; revised manuscript received December 23, 2002, accepted December 27, 2002.

Abbreviations and Acronyms

CRT	= cardiac resynchronization therapy
DCM	= dilated cardiomyopathy
FDG	= ^{18}F -fluorodeoxyglucose
HF	= heart failure
LBBB	= left bundle branch block
LV	= left ventricular
LVEDV and LVESV	= left ventricular end-diastolic and end-systolic volume, respectively
LVEF	= left ventricular ejection fraction
PET	= positron emission tomography
SPECT	= single-photon emission computed tomography
$^{99\text{m}}\text{Tc}$	= technetium-99m

METHODS

Patients. We investigated 15 patients with DCM (10 females; age 61 ± 13 years; body weight 73 ± 14 kg) with HF (all in New York Heart Association functional class III) and LBBB. All patients were in sinus rhythm with a mean PR interval of 200 ± 41 ms (range 165 to 310) and a mean QRS width of 165 ± 15 ms (range 140 to 200). Coronary artery disease was ruled out in all patients by preoperative coronary angiography. Patients received a resynchronization pacemaker for biventricular ($n = 13$) or LV ($n = 2$) pacing. Left ventricular pacing leads were positioned in a lateral ($n = 12$) or anterolateral position ($n = 3$). The mean programmed atrioventricular delay was 105 ± 17 ms.

Patients were examined with FDG-PET and $^{99\text{m}}\text{Tc}$ -sestamibi SPECT immediately before and 14 days after CRT initiation. They fasted on the study days and received optimized medical HF treatment, which was unchanged during the entire study.

The study was approved by the institutional Review Committee, and patients gave written, informed consent to participate in the trial.

FDG-PET. To reduce myocardial fatty acid metabolism and stimulate insulin-dependent glucose uptake, all patients received 250 mg acipimox 2 h and 50 g glucose orally 1 h before administration of FDG. Gated FDG-PET scans (ECAT EXACT 922/47, Siemens-CTI, Knoxville, Tennessee) were performed 60 min after intravenous administration of 284 ± 30 MBq FDG, with eight gates per RR interval. The acquisition time was 30 min for emission (two-dimensional mode) and 15 min for transmission ($^{68}\text{Ge}/^{68}\text{Ga}$ rod sources). The eight sinograms of the gated acquisition were added up to create one ungated sinogram, and attenuation-corrected gated and ungated images were reconstructed using an iterative algorithm (Ordered Subsets Expectation Maximization [OSEM], 16 subsets, 6 steps). For ungated and gated images, the matrix size was 128×128 pixels and 64×64 pixels and the reconstruction zoom was 2.15 and 1.78, respectively.

$^{99\text{m}}\text{Tc}$ -sestamibi SPECT. Myocardial perfusion SPECT imaging was performed 60 min after injection of 424 ± 17

MBq $^{99\text{m}}\text{Tc}$ -sestamibi, with a light meal after tracer application. Data were acquired using a dual-head gamma camera (Solus, ADAC Laboratories, Milpitas, California). Acquisition parameters, attenuation- and scatter-corrected reconstruction in a 128×128 matrix were described in detail elsewhere (11). Briefly, emission was performed in three independent energy windows: 140 ± 14 keV for emission, 120 ± 6 keV for scatter detection, and 90 ± 11 keV for backscatter detection. Data sets of windows 1 and 2 were processed to obtain a scatter-corrected data set, which was then reconstructed using a Butterworth filter (cutoff 0.7 Nyquist, order of 5, matrix 128×128) and processed with the data set of window 3 (filtered backprojection, Ramp 0.5) to obtain a final segmented attenuation- and scatter-corrected transaxial data set.

PET and SPECT analyses. Ungated FDG and $^{99\text{m}}\text{Tc}$ -sestamibi images were reoriented according to the LV axes. Relative distributions of myocardial FDG and $^{99\text{m}}\text{Tc}$ -sestamibi uptake values were assessed using a volumetric vector sampling method in 25 segments. Segmental FDG and $^{99\text{m}}\text{Tc}$ -sestamibi uptake was displayed as the percentage of the segment with peak activity. Mean FDG and $^{99\text{m}}\text{Tc}$ -sestamibi uptake of four LV wall areas (septal, anterior, lateral, and posterior)—each consisting of six segments—was calculated as the mean value of the respective six segments for every patient. Due to possible ambiguous assignment, the remaining apical segment was not included in the wall area analysis. The septal-to-lateral ratios were determined as septal FDG or $^{99\text{m}}\text{Tc}$ -sestamibi uptake divided by the uptake values of the lateral wall. Figure 1 displays representative examples of FDG-PET and $^{99\text{m}}\text{Tc}$ -sestamibi SPECT images, as well as individual uptake values, at baseline and during CRT in a 50-year-old female patient with severe LV dilation due to nonischemic cardiomyopathy.

The pixel size of gated FDG images was changed to an isotropic pixel size of 5.79 mm. These data were reoriented and analyzed for LV end-diastolic (LVEDV) and end-systolic volumes (LVESV), as well as for LVEF, with the software tool called Quantitative Gated SPECT (QGS, Cedars-Sinai Medical Center, California).

Statistics. Statistical analyses were performed using SPSS version 10 (SPSS Inc., Chicago, Illinois). Data are expressed as the mean value \pm SD. Dependencies of tracer uptake on the different myocardial wall areas (i.e., differences of relative FDG and $^{99\text{m}}\text{Tc}$ -sestamibi uptake values between septal, anterior, lateral, and posterior myocardium) were analyzed using the nonparametric Kruskal-Wallis test. This test was performed separately for both baseline and CRT examinations. Differences between wall areas in their responses over time, in terms of FDG or $^{99\text{m}}\text{Tc}$ -sestamibi uptake values, were also assessed with the Kruskal-Wallis test.

Intragroup comparisons (i.e., differences of mean values before and during CRT) were tested for significance using a nonparametric test for paired samples (Wilcoxon). Statisti-

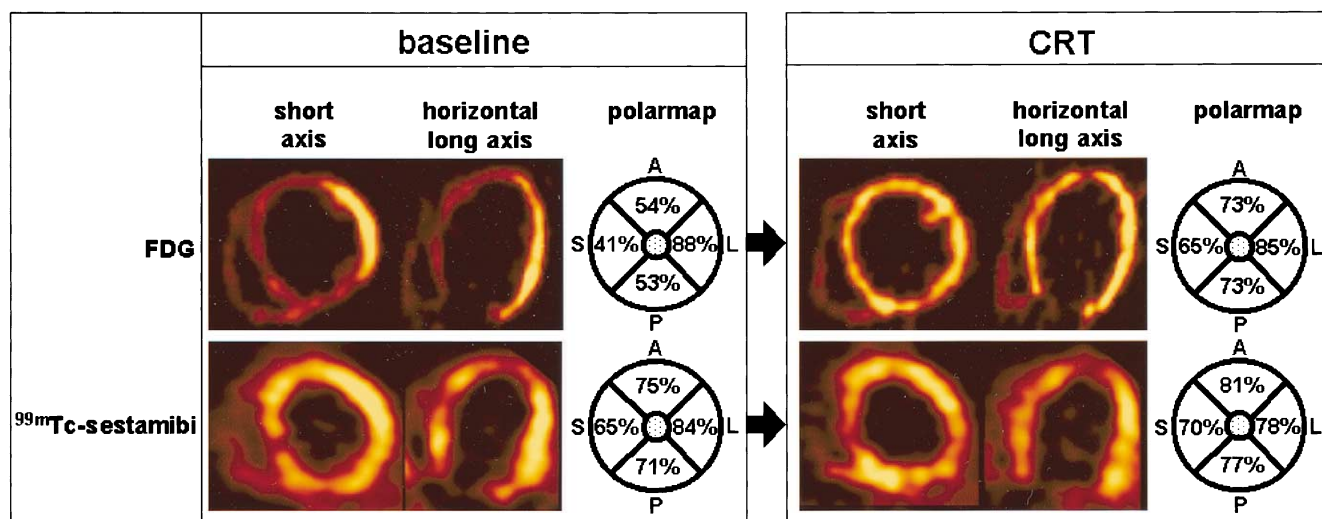


Figure 1. Example of ^{18}F -fluorodeoxyglucose-positron emission tomography and technetium-99m-sestamibi single-photon emission computed tomography images at baseline and during cardiac resynchronization therapy in a 50-year-old female patient with severe left ventricular dilation due to nonischemic cardiomyopathy. Shown are representative short-axis and horizontal long-axis slices of 1.2 cm thickness, as well as individual uptake values of the respective wall areas. A = anterior wall area; L = lateral wall area; P = posterior wall area; S = septal wall area.

cal analyses of differences between FDG and $^{99\text{m}}\text{Tc}$ -sestamibi in their uptake values, septal-to-lateral ratios and corresponding changes over time were performed with a nonparametric test for independent samples (Mann-Whitney U test). A p value <0.05 was considered significant.

RESULTS

Impact of CRT on myocardial glucose metabolism and perfusion. At baseline, glucose metabolism in patients with DCM and LBBB showed significant differences between the analyzed myocardial wall areas ($p < 0.0001$). Uptake was highest in the lateral wall and lowest in the septum, with intermediate values for the anterior and posterior wall (Fig. 2A). Myocardial perfusion also showed significant differences between the respective wall areas ($p < 0.0001$), although these were less marked than differences in glucose metabolism (Fig. 2B).

$^{99\text{m}}\text{Tc}$ -sestamibi uptake was significantly higher than FDG uptake in the septum ($65 \pm 10\%$ vs. $56 \pm 12\%$, $p < 0.05$) and lower in the lateral wall ($84 \pm 5\%$ vs. $89 \pm 6\%$, $p < 0.01$). Accordingly, the mean septal-to-lateral ratio at baseline was significantly lower for FDG (0.62 ± 0.12) than for $^{99\text{m}}\text{Tc}$ -sestamibi (0.77 ± 0.13 , $p < 0.001$) (Figs. 2A and 2B).

During CRT, wall areas showed significantly different responses in their FDG uptake ($p < 0.0001$) and $^{99\text{m}}\text{Tc}$ -sestamibi uptake ($p < 0.01$). Glucose metabolism increased significantly by 25% in the septum and 17% in the anterior wall, whereas metabolism decreased significantly by 11% in the lateral wall. Thus, glucose metabolism was homogeneously distributed in the LV myocardium and mean FDG uptake values did not differ between the respective wall areas ($p = 0.128$) (Fig. 2A). The influence of CRT on regional

myocardial perfusion was less pronounced. Relative $^{99\text{m}}\text{Tc}$ -sestamibi uptake increased by 6% in the septum and 8% in the anterior wall. A reduced spatial heterogeneity of myocardial perfusion between the respective wall areas ($p < 0.05$) remained, with lowest $^{99\text{m}}\text{Tc}$ -sestamibi uptake in the septum and highest uptake in the lateral wall (Fig. 2B).

Consequently, mean septal-to-lateral ratios for FDG and $^{99\text{m}}\text{Tc}$ -sestamibi both increased significantly to 0.91 ± 0.26 ($p < 0.001$) and 0.85 ± 0.16 ($p < 0.01$), respectively, although the relative increase was significantly ($p < 0.0001$) higher for FDG (47%) than for $^{99\text{m}}\text{Tc}$ -sestamibi (10%) (Figs. 2A and 2B).

When the two patients with LV pacing were compared with the 13 patients paced in the biventricular mode, both baseline FDG and $^{99\text{m}}\text{Tc}$ -sestamibi uptake values and changes during CRT were comparable between both pacing modes. Uptake values of FDG and $^{99\text{m}}\text{Tc}$ -sestamibi before and during CRT in the two LV-paced patients were also substantively similar to those in all 15 patients.

Impact of CRT on LV function. At baseline, mean LVEDV and LVESV were 293 ± 160 and 244 ± 164 ml, respectively. After two weeks of CRT, LVEDV decreased significantly to 272 ± 158 ml ($p < 0.05$) and LVESV to 220 ± 160 ml ($p < 0.01$). Mean LVEF increased from $22 \pm 12\%$ at baseline to $25 \pm 13\%$ after CRT ($p < 0.01$).

DISCUSSION

Cardiac resynchronization therapy has been proposed as an adjunctive treatment for patients with severe HF and LBBB. Short-term hemodynamic (9,10,12) and long-term functional improvements have been reported (13–15). The benefit of CRT is achieved by improved chamber efficiency, as demonstrated by a reduction in myocardial energy consumption (16). Moreover, a reduction in LV volumes after

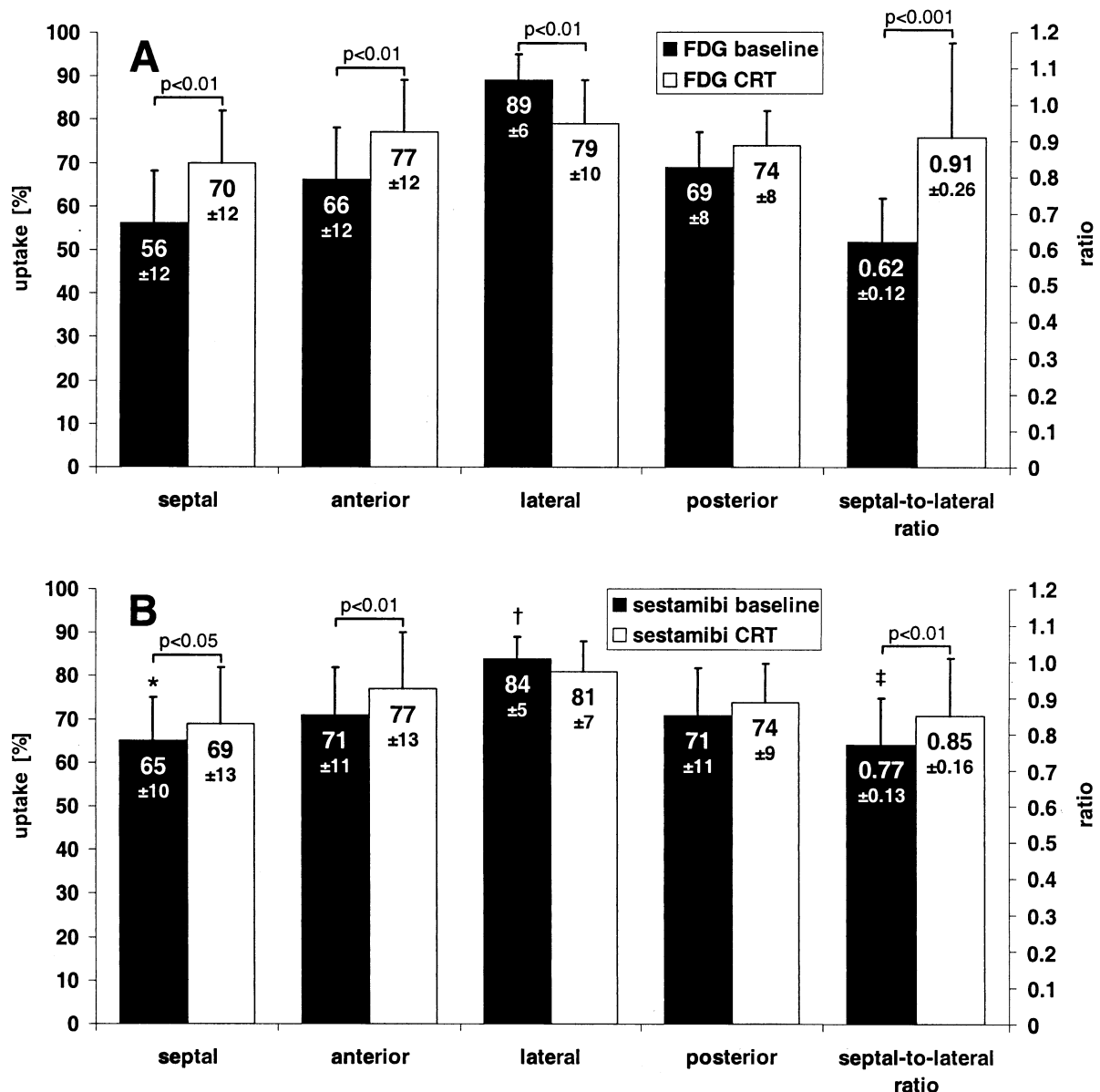


Figure 2. Mean (\pm SD) relative ^{18}F -fluorodeoxyglucose (FDG) (A) and technetium-99m-sestamibi (B) uptake values of the four left ventricular wall areas, as well as septal-to-lateral ratios at baseline and during cardiac resynchronization therapy (CRT) in 15 patients. *p < 0.05, †p < 0.01, and ‡p < 0.001 compared with FDG.

CRT has been observed in echocardiographic studies (17,18).

Resynchronization of LV contraction by advancing LV free wall activation has been implicated as one major mechanism of CRT (19). The extent of the LV base displaying delayed longitudinal contraction, as detected by echocardiographic tissue Doppler imaging, has been shown to predict the long-term efficacy of CRT. With tissue tracking, improved regional longitudinal systolic shortening during CRT could be demonstrated (20). Near-simultaneous contraction of the septum and LV free wall may lead to septal reloading during LV systole. This is underscored by data provided by Kawaguchi et al. (21), who used contrast-enhanced echocardiography to show that one

major mechanism of hemodynamic improvement with CRT is an increase in septal inward motion. With the same technique, these authors could also show a 40% reduction of LV dyssynchrony with CRT.

The main finding of our study is that the reduction of mechanical LV dyssynchrony by CRT is accompanied by homogenization of the unbalanced cardiac glucose metabolism in DCM and LBBB, with less influence on myocardial perfusion. Previous studies have shown a reduction in septal glucose metabolism in patients with LBBB (2,22). In contrast, results on resting perfusion abnormalities in LBBB have not uniformly demonstrated a reduction in septal perfusion (2,4-8,23). The results of our study indicate that septal glucose metabolism is more reduced than perfusion,

which is in good agreement with the postulated septal reverse perfusion/glucose metabolism mismatch in LBBB (2,22).

The most likely explanation for reduced septal glucose uptake in LBBB is therefore a perfusion-independent specific alteration of transmembranous glucose transport and/or the subsequent phosphorylation kinetics (24). This is underscored by previous evidence for preserved septal viability and metabolic activity associated with beta-oxidation and oxygen consumption, as determined with the ^{18}F -labeled fatty acid 14(R,S)- ^{18}F -fluoro-6-thia-heptadecanoic acid and with ^{11}C -acetate in LBBB (25,26).

There is experimental evidence that early septal contraction against the relaxed LV free wall in LBBB reduces septal work load, because pressure is still low and no ejection occurs (27). On the other hand, late activation of the LV lateral wall in patients with LBBB occurs at higher stress, because the earlier activated septum has already developed tension (21,28). Our data indicate that these known alterations in ventricular mechanics result in corresponding changes in myocardial glucose metabolism, as indicated by the diminished baseline septal-to-lateral ratio of FDG uptake.

Theoretically, reduced septal work load would entail decreasing adenosine triphosphate requirements of the septum, with concomitantly diminished glucose metabolism (3). Depre et al. (29) provided indirect evidence for this hypothesis by an animal model of unloaded rat hearts being transplanted on the abdominal aorta of isogenic recipients. Gene expression for the insulin-sensitive glucose transporter GLUT-4 in these hearts decreased one day after transplantation, resulting in myocardial insulin resistance, characterized by a reduction of insulin-dependent myocardial glucose oxidation in unloaded hearts (30). This flexible regulation of cardiomyocyte gene expression could provide the pathophysiologic basis for alterations in septal glucose metabolism in the sense of septal insulin resistance in patients with HF and LBBB, which is reversed by CRT. Indeed, rapid re-expression of GLUT-4 occurred within 60 min when the energy needs increased upon reloading of rat hearts (29).

Myocardial glucose metabolism in this study was measured after an oral glucose load, which is a stimulus for insulin release. Thus, the observed reduction in septal glucose metabolism and its reversal with CRT in our study are well in accordance with the results on GLUT-4 messenger ribonucleic acid expression and insulin resistance observed in the model of unloaded and reloaded rat hearts (29,30).

Conclusions. Glucose metabolism is reduced to a greater extent than perfusion in the septum and adjacent anterior and posterior LV wall in patients with DCM and LBBB. The hemodynamic benefit of CRT is paralleled by restoration of homogeneous myocardial glucose metabolism, with less influence on perfusion.

Reprint requests and correspondence: Dr. Bernd Nowak, Department of Nuclear Medicine, University Hospital Aachen, Pauwelsstrasse 30, 52074 Aachen, Germany. E-mail: bnowak@ukaachen.de.

REFERENCES

1. Ono S, Nohara R, Kambara H, Okuda K, Kawai C. Regional myocardial perfusion and glucose metabolism in experimental left bundle branch block. *Circulation* 1992;85:1125-31.
2. Zanco P, Desideri A, Mobilia G, et al. Effects of left bundle branch block on myocardial FDG PET in patients without significant coronary artery stenoses. *J Nucl Med* 2000;41:973-7.
3. Bassingthwaite JB, Li Z. Heterogeneities in myocardial flow and metabolism: exacerbation with abnormal excitation. *Am J Cardiol* 1999;83:7H-12H.
4. Delonca J, Camenzind E, Meier B, Righetti A. Limits of thallium-201 exercise scintigraphy to detect coronary disease in patients with complete and permanent bundle branch block: a review of 134 cases. *Am Heart J* 1992;123:1201-7.
5. Jukema JW, van der Wall EE, van der Vis-Melsen MJ, Kruyswijk HH, Bruschke AV. Dipyrindamole thallium-201 scintigraphy for improved detection of left anterior descending coronary artery stenosis in patients with left bundle branch block. *Eur Heart J* 1993;14:53-6.
6. Althoefer C, vom Dahl J, Kleinhans E, Uebis R, Hanrath P, Buell U. ^{99m}Tc -methoxyisobutylisonitrile stress/rest SPECT in patients with constant complete left bundle branch block. *Nucl Med Commun* 1993;14:30-5.
7. Patel R, Bushnell DL, Wagner R, Stumbris R. Frequency of false-positive septal defects on adenosine/ ^{201}Tl images in patients with left bundle branch block. *Nucl Med Commun* 1995;16:137-9.
8. Lebtahi NE, Stauffer JC, Delaloye AB. Left bundle branch block and coronary artery disease: accuracy of dipyrindamole thallium-201 single-photon emission computed tomography in patients with exercise anteroseptal perfusion defects. *J Nucl Cardiol* 1997;4:266-73.
9. Kass DA, Chen CH, Curry C, et al. Improved left ventricular mechanics from acute VDD pacing in patients with dilated cardiomyopathy and ventricular conduction delay. *Circulation* 1999;99:1567-73.
10. Auricchio A, Stellbrink C, Block M, et al., the Pacing Therapies for Congestive Heart Failure Study Group and the Guidant Congestive Heart Failure Research Group. Effect of pacing chamber and atrio-ventricular delay on acute systolic function of paced patients with congestive heart failure. *Circulation* 1999;99:2993-3001.
11. Kupferschlag J, Muller B, Schulz G, et al. A method for combined scatter and attenuation correction without transmission measurement for myocardial SPECT with ^{99m}Tc binding. *Nuklearmedizin* 1997;36:56-64.
12. Leclercq C, Cazeau S, Le Breton H, et al. Acute hemodynamic effects of biventricular DDD pacing in patients with end-stage heart failure. *J Am Coll Cardiol* 1998;32:1825-31.
13. Cazeau S, Leclercq C, Lavergne T, et al. Effects of multisite biventricular pacing in patients with heart failure and intraventricular conduction delay. *N Engl J Med* 2001;344:873-80.
14. Abraham WT, Fisher WG, Smith AL, et al. Cardiac resynchronization in chronic heart failure. *N Engl J Med* 2002;346:1845-53.
15. Auricchio A, Stellbrink C, Sack S, et al. Long-term clinical effect of hemodynamically optimized cardiac resynchronization therapy in patients with heart failure and ventricular conduction delay. *J Am Coll Cardiol* 2002;39:2026-33.
16. Nelson GS, Berger RD, Fetters BJ, et al. Left ventricular or biventricular pacing improves cardiac function at diminished energy cost in patients with dilated cardiomyopathy and left bundle-branch block. *Circulation* 2000;102:3053-9.
17. Stellbrink C, Breithardt OA, Franke A, et al. Impact of cardiac resynchronization therapy using hemodynamically optimized pacing on left ventricular remodeling in patients with congestive heart failure and ventricular conduction disturbances. *J Am Coll Cardiol* 2001;38:1957-65.
18. Saxon LA, De Marco T, Schafer J, Chatterjee K, Kumar UN, Foster E. Effects of long-term biventricular stimulation for resynchronization

- on echocardiographic measures of remodeling. *Circulation* 2002;105:1304-10.
19. Butter C, Auricchio A, Stellbrink C, et al. Effect of resynchronization therapy stimulation site on the systolic function of heart failure patients. *Circulation* 2001;104:3026-9.
20. Sogaard P, Egeblad H, Kim WY, et al. Tissue Doppler imaging predicts improved systolic performance and reversed left ventricular remodeling during long-term cardiac resynchronization therapy. *J Am Coll Cardiol* 2002;40:723-30.
21. Kawaguchi M, Murabayashi T, Fetters BJ, et al. Quantitation of basal dyssynchrony and acute resynchronization from left or biventricular pacing by novel echo-contrast variability imaging. *J Am Coll Cardiol* 2002;39:2052-8.
22. Althoefer C, vom Dahl J, Buell U. Septal glucose metabolism in patients with coronary artery disease and left bundle-branch block. *Coron Artery Dis* 1993;4:569-72.
23. Sugihara H, Tamaki N, Nozawa M, et al. Septal perfusion and wall thickening in patients with left bundle branch block assessed by technetium-99m-sestamibi gated tomography. *J Nucl Med* 1997;38:545-7.
24. Althoefer C. LBBB: challenging our concept of metabolic heart imaging with fluorine-18-FDG and PET? *J Nucl Med* 1998;39:263-5.
25. Althoefer C, vom Dahl J, Bares R, Stocklin GL, Bull U. Metabolic mismatch of septal beta-oxidation and glucose utilization in left bundle branch block assessed with PET. *J Nucl Med* 1995;36:2056-9.
26. Zanco P, Chierichetti F, Fini A, Cargnel S, Ferlin G. Myocardial perfusion, glucose utilization and oxidative metabolism in a patient with left bundle branch block, prior myocardial infarction and diabetes. *J Nucl Med* 1998;39:261-3.
27. Prinzen FW, Hunter WC, Wyman BT, McVeigh ER. Mapping of regional myocardial strain and work during ventricular pacing: experimental study using magnetic resonance imaging tagging. *J Am Coll Cardiol* 1999;33:1735-42.
28. Nelson GS, Curry CW, Wyman BT, et al. Predictors of systolic augmentation from left ventricular preexcitation in patients with dilated cardiomyopathy and intraventricular conduction delay. *Circulation* 2000;101:2703-9.
29. Depre C, Shipley GL, Chen W, et al. Unloaded heart in vivo replicates fetal gene expression of cardiac hypertrophy. *Nat Med* 1998;4:1269-75.
30. Doenst T, Goodwin GW, Cedars AM, Wang M, Stepkowski S, Taegtmeier H. Load-induced changes in vivo alter substrate fluxes and insulin responsiveness of rat heart in vitro. *Metabolism* 2001;50:1083-90.